Numerical Simulation of Push-and-Release Tests of Hybrid Isolation Systems

Numerical simulation of push-and-release tests of hybrid isolation systems

Fabio Micozzi [0000-0001-8651-670X]1, Alberto Poeta[1], Laura Gioiella [0000-0002-9211-6830]1, Laura Ragni[0000-0003-0256-358X]2 and Andrea Dall'Asta [0000-0001-7482-9434]1

[1] School of Architecture and Design, University of Camerino, Ascoli Piceno (AP), Italy
[2] Department of Civil and Building Engineering and Architecture, Polytechnic University of Marche, Ancona (AN), Italy

fabio.micozzi@unicam.it

Abstract. This study illustrates the comparison between the experimental testing of a two-storey braced-frame structure semically protected by means of and isolation system and the simulation of such tests. More in detail, the steel structure rests on a reinforced concrete slab isolated from the foundations through a hybrid system consisting of 28 High-damping Rubber Bearings (HDRBs) and 36 low-friction sliders (LFSs). During the building design the removable push-and-release device, the reaction wall, and the pushing point were also designed to minimize the cost of the tests and to allow repeated testing throughout the service life of the building. The global dynamic response was tested up to displacement amplitudes similar to those induced by extreme seismic events. In particular, maximum horizontal displacements of 285 mm and 227 mm in the quasi-static and dynamic tests are reached respectively. Conseqeuntly, the test can be de-facto considered as an in-situ verification of the seismic behaviour of the isolation system. However, in the case case of elastomeric bearings this testing procedure is not properly equivalent to an earthquake excitation, mainly due to the different deformation velocities and the not negligible viscous effects of HDRBs. Therefore, this work aims at understanding and evaluating the observed experimental behaviour by assessing and calibrating a model able to simulate all the the viscous effects and the energy dissipated by the sliders. This way, the viscous displacement accumulated during the loading phase, causing the system to oscillate around a non zero displacement during the release phase, can be simulated.

Keywords: Push-and-Release tests, hybrid seismic isolation, high damping rubber bearings, viscous effects.

1 Introduction

Due to the primary role of isolation bearings on the seismic response of base-isolated structures, seismic design codes require rigorous qualification and quality production control tests to evaluate the actual properties of the devices and demonstrate the compliance with the design requirements. However, a reduced number of devices is usually tested during quality control, as prescribed by the codes as a function of the device type. For example, the European code EN 15129 [1] prescribes that 20% of isolation bearings (HDRBs) must be tested, while one device per production lot, constituted by maximum 20 devices, must be tested in the case of Concave Surface sliders (CCSs). Moreover, for hybrid isolation systems, where Low Friction Sliding Bearings (LFSBs) are used together HDRBs, LFSBs are usually used only as vertical supports. In this case the conformity to the code EN 1337 [2] does not include tests to verify the effective friction coefficient on the full-scale bearing. Qualification and control tests according EN 15129 [1] are mandatory only in the case that LFSBs are used also to dissipate energy. Therefore, in-situ tests carried out on base-isolation structures may be strategic to verify the actual behaviour of the whole isolation system in the installed condition, including not only HDRBs but also the LFSBs.

This study illustrates the experimental testing of a two-storey (5875 m^2) steel braced-frame structure semically protected by means of an hybrid isolation system. More in detail, the steel structure rests on a reinforced concrete slab isolated from the foundations through a hybrid system consisting of 28 High-damping Rubber Bearings (HDRBs) and 36 low-friction sliders (LFSs). During the building design the removable push-and-release device, the reaction wall, and the pushing point are also designed to minimize the cost of the tests and allows for repeated testing throughout the service life of the building. The global dynamic response was tested up to displacement amplitudes similar to those induced by extreme seismic events. In particular maximum horizontal displacements of 285 mm and 227 mm in the quasi-static and dynamic tests are reached respectively, thus they can be considered as an in-situ verification of the seismic behaviour of the isolation system. However, in the case case of HDRBs this testing procedure is not properly equivalent to an earthquake excitation, mainly due to three reason: *i)* the loading phase is pseudo-static, *ii)* the dynamic phase (after the sudden release of the building) is mainly related to the elastic energy accumulated by the bearings during the loading phase and *iii)* the stiffness and damping of high damping rubber bearings may be influenced by the slow loading path due to the viscous component. Therefore, this work aims at understanding the experimental behaviour by assessing and calibrating a model able to simulate all the viscous effects of the HDRBs as weel as the energy dissipated by the LFBSs. By this way, the over-damped cyclic behaviour can be simulated as well as the viscous displacement accumulated during the loading phase, causing the system to oscillate around a non zero displacement during the release phase.

2 Tested building

The tested building is the new research centre of the University of Camerino, a strategic building hosting very sensitive instruments of the chemistry and physics laboratories. Its construction was funded by the Italian Department of Civil Protection (DPC) after the 2016-2017 Central Italy seismic sequence that severely damaged many of the facilities of the University of Camerino. The building is also intended to work as coordination centre of the DPC during future post-earthquake emergency phases. Construction works began in July 2019, structures were completed in June

2020, the tests here described were made in July 2020, inauguration took place in July 2021.

The superstructure is a steel braced frame with pinned joints, designed using a 7.2 m × 7.2 m modular system, for a total of 7 modules along each direction, plus a cantilever zone spanning 1.9 m along the entire perimeter of the building (Fig.1), accordingly, floors are 54.20 m × 54.20 m. Four concentric inverted-V braces were adopted along each principal direction. The substructure was designed to adapt to the morphology of the area characterized by a remarkable slope, resulting in reinforced concrete (RC) foundations with a complex yet regular geometry and RC rigid columns connecting the deeper foundation levels to the isolation level.

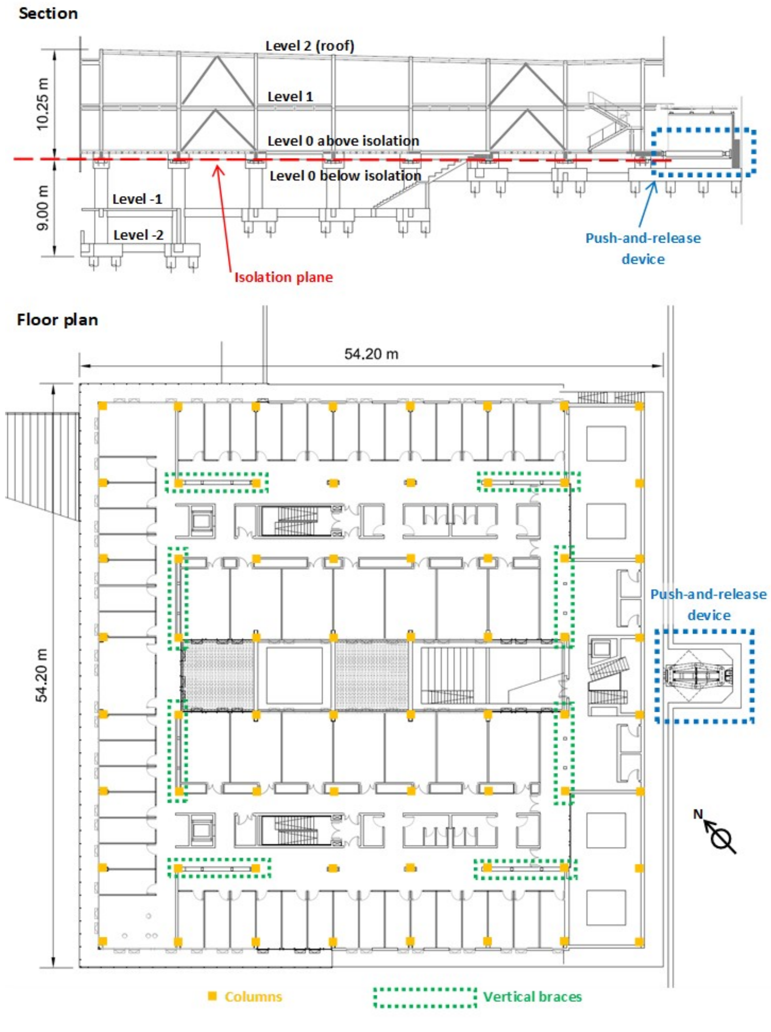

Fig. 1. Tested building in Camerino, Italy.

The isolation system consists of 28 HDRBs arranged on the perimeter to maximize torsional stiffness, and 36 LFSBs in the central part to support the higher vertical loads. It has been designed according to general criteria described in [3] and by assuming an isolation period $T_{is} = 3.60$ s, to guarantee the absence of damage on the superstructure and its content up to the maximum design action. HDRBs have diameter 600 mm, total height of rubber 184 mm, horizontal rigidity 0.62 kN/mm, maximum displacement 350 mm (shear deformation about 200%). This displacement capacity is slightly larger than the displacement demand required at the Collapse Limit State (CLS), return period $R_P = 1950$ years, which is 324 mm with torsional effects included. In their design, a damping ratio equal to 10% and a shear stiffness equal to 0.4 MPa (soft rubber) were assumed. LFSBs have a 400 mm displacement capacity and a dynamic friction coefficient lower than 1% at the seismic vertical force condition. Type tests and factory production tests carried out before and after the devices production confirmed the design assumption, except for the damping ratio equal to 14 %, as provided by the manufacturer. Further information regarding the design process can be found in [4].

3 Push-and-release device and testing set-up

The push-and-release device consists of a quadrilateral articulated steel system (Fig.2) and relevant contrasting structures. Two hydraulic jacks with maximum stroke of 300 mm and total maximum force of 10 MN and two load cells were positioned in series with the quadrilateral system. A sacrificial steel rod made of high strength steel is inserted in the middle of the tie element of the quadrilateral system, working as a fuse. The strut angle respect to the pushing direction defines the ratio between the pushing force and the tension force applied to the fuse. The high accuracy of the release force is ensured by the small plastic deformation of high strength steel used for the fuse and by its shape which ensures a brittle rupture of the rod. When the fuse breaks, the base-isolated building starts to oscillate in free-vibration conditions. It is remarked that both the push-and-release device mass and friction force are negligible with respect to the building mass and reaction force. The push-and-release device may be used to repeat the tests during the building life to investigate the aging effect in HDRBs. The building was equipped with sixteen uniaxial piezoelectric accelerometers: five at level 0, four at level 1, four at the roof, and the remaining close to three. Strain gauges were also applied to two adjacent steel braces at level 0 and to the corresponding two steel braces at level 1. Four linear displacement transducers were installed to monitor horizontal displacements: three at the isolation level (Fig.3a) and one at level 1 between the floor slab and the retaining wall external to the base isolation. Two contactless inductive distance sensors were used to monitor vertical displacements by placing a rectified 15 mm thick steel plate connected to the fixed base as target surface (Fig.3b). Finally, the environmental conditions (temperature and RH) were also recorded through three standalone digital sensors. In this paper only data from displacement transducers at the isolation level are analysed. Further information regarding the other experimental data processing can be found in [5]

Fig. 2. Articulated steel system and reaction wall constituting the push-and-release device.

(a) (b)

Fig. 3. Configuration and installation of displacement sensors at level 0 in the horizontal (a) and vertical (b) directions.

4 Experimental results

The experimental tests were performed when the stell structure was completed, but without partitions, external walls, architectural elements, and technological equipment. The total estimated mass of the structures above the isolators was 4633 tons. Two types of push-and-release tests were made: 1) loading and unloading without sudden release, hereafter called quasi-static (S) tests; 2) loading up to the rupture of the fuse followed by a sudden release, hereafter called dynamic (D) tests. The sequence of the tests is reported in Table 1, with indication of the starting time, the duration of the loading phase for quasi-static and dynamic tests, the maximum horizontal force and displacement. The amplitude of displacements ranged from 109.4 mm to 284.6 mm, being the higher value close to the maximum displacement of the isolation system expected at the CLS. In the first test no displacements were recorded as the applied horizontal force was lower than the breakaway friction force.

Table 1. Tests sequence.

	Test	Starting time	Duration [min]	Max force [kN]	Max displacement [mm]
3rd July 2020	S1	12:22	6	518	0.0
	D1	13:47	16	2729	177.3
	S2	16:36	21	3206	232.4
6th July 2020	D2	12:24	8	1756	109.4
	D3	13:36	18	3122	226.9
	D4	15:56	9	1786	121.8
	S3	17:07	25	3834	284.6

The displacement time-histories during both dynamic and static tests are reported in Fig.4a. In the quasi-static tests, the time was set to zero when the displacement decrement started. In the dynamic tests, the time was set to zero when the load cells recorded the drop of the applied horizontal force due to collapse of the fuse. The transducers monitoring the horizontal displacements in the testing direction gave the same synchronized readings during both the push and release phases, thus, indicating absence of rotations with respect to the vertical axis. The transducer monitoring the displacement perpendicular to the testing direction confirmed that no transverse movement was activated. Fig. 4b shows a zoom of the release phase of dynamic tests is shown, where the free vibration motion of the building can be observed. It is evident from the recorded responses that the system oscillates around a non zero displacement during the release phase following a high-damped cyclic behaviour.

Fig.5a shows the horizontal force-displacement curves in the loading and unloading phases. For dynamic tests the force during the release have been derived from the acceleration recorded at the isolation level and the mass of the structure. In test D1 the structure was moved for the first time from its initial position and a breakaway friction force equal to 700 kN was reached. In the subsequent tests, smaller values of the breakaway friction force were found. Given that the trajectory followed in all the tests was the same, the lubrification of the sliding surfaces increased test after test, in accordance with phenomena already observed in [6]. It is also remarked that the building did not start from the initial position in the tests following D1, as can been seen in Fig.4 where the ordinates do not drop to zero at the end of the tests (residual horizontal displacements). Accordingly, the initial force measured to start the movement was not only related to the friction of LFSBs but also to the residual force of HDRBs. Test D1 is also influenced by the first cycle effect of the virgin rubber, i.e., the first time that the HDRBs reach this level of strain [7-13] thus all the tests are substantially overlapping except for D1. Moreover, it is worth to note that t unloading branches of dynamic tests are significantly different from the static ones because of the different velocity involved. Thus, the larger viscous component of the rubber strongly increases the energy dissipated during the dynamic tests.

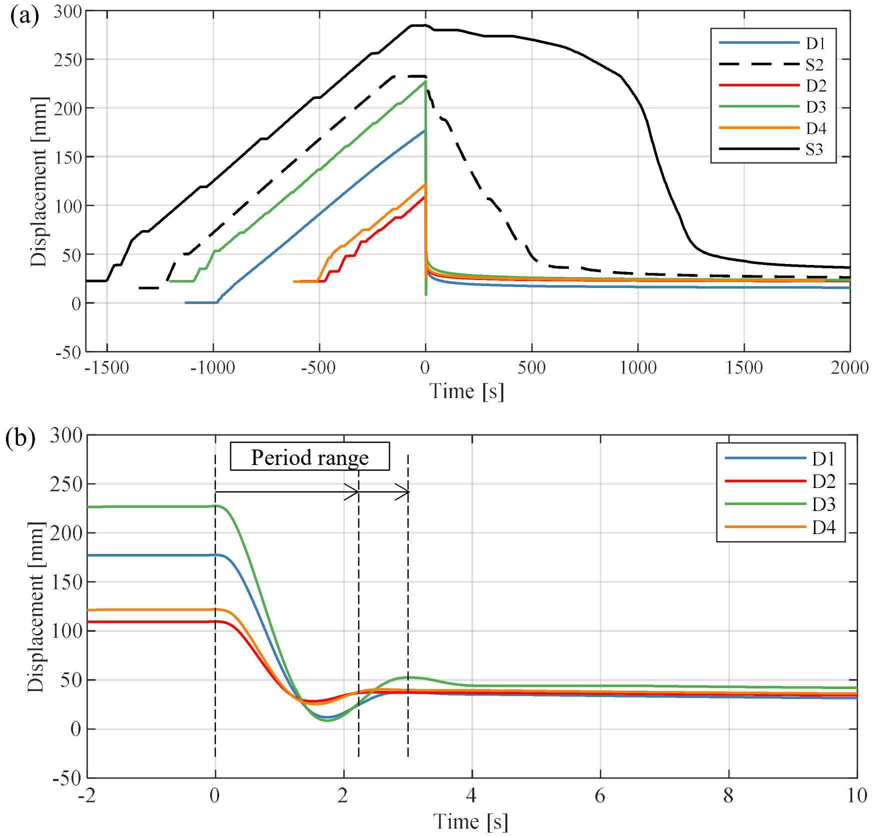

Fig. 4. Displacement time-history curves of the dynamic and static tests (a) and dynamic tests during the release phase (b).

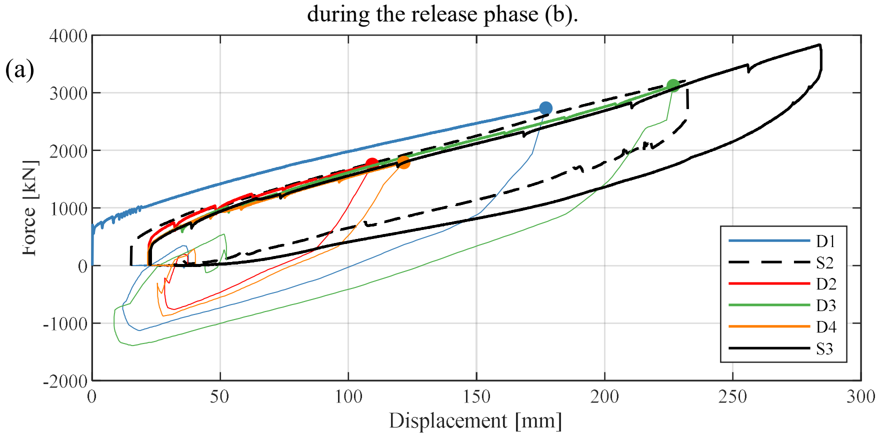

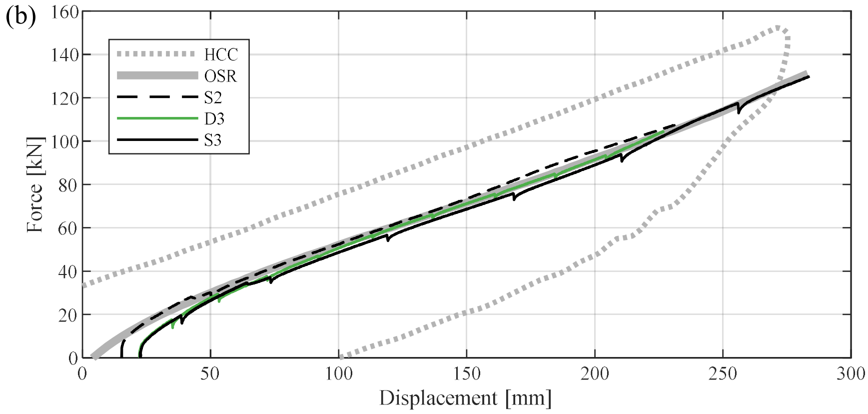

Fig. 5. Force-displacement curves of the dynamic and static tests.

Fig. 5b shows the loading ramp of the tests with largest displacements (S2, D3 and S3), once deducted of the dynamic friction force (200 kN) previously estimated and scaled with respect to a single HDRB. This allows to compare the obtained experimental curves with the control tests carried out on some isolators before their installation. Specifically, the loading ramp of the One Side Ramp (OSR) test and the third cycle of the Horizontal Cyclic Characteristic (HCC) test at 150 % of shear deformation are reported. It is observed the full agreement between the experimental curves and the OSR test (both in the quasi-static range of load velocity), confirming the correctness of the global stiffness of the HDRBs and the negligible viscous overstresses generated by the rubber in this range of velocities. On the contrary, in the dynamic range of velocity the viscous behavior of this kind of rubber leads to a significant strain-rate dependent behavior as shown by the HCC test (performed in laboratory at 0.5 Hz, with a mean speed of 550 mm/s).

5 Numerical simulation

To simulate the response of the isolation system a SDOF (Single-Degree-Of-Freedom-Model) model has been adopted, by neglecting the deformability of the steel superstructure and r.c. substructure. This model is quite simple, but it is adequate to catch the most relevant phenomena involved in the response to the push-and-release test, mainly related to the viscous deformation cumulated during the loading phase. As concern the isolation system, the model consists of three in-parallel elements (Fig.6): a Kelvin model characterized by the stiffness k_0 and the damping constant c_0, a Maxwell model characterized by the stiffness k_1 and the damping constant c_1 and a friction model characterized by the friction force F_{fr}. The first two elements simulate the response of HDRBs, while the latter represents the contribution of LFSs. More in detail, the Kelvin model describes the viscoelastic response with short relaxation time (short term viscosity), while the Maxwell model describes the viscous contribution with long relaxation time (long term viscosity), as already experimentally observed and implemented in more complex models [6-11].

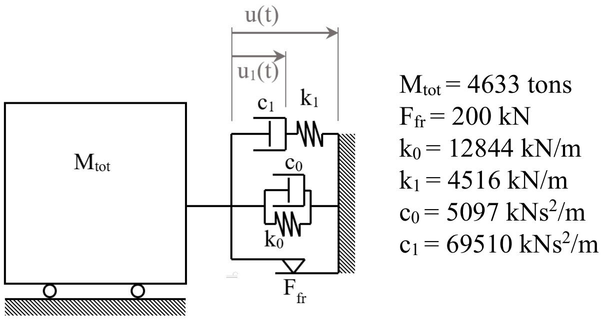

Fig. 6. Numerical model of the isolation system

Test D3 was used to calibrate the viscoelastic parameters (k_0, c_0, k_1 and c_1), while the dynamic friction force can be obtained directly from the force-displacement diagram of the quasi-static tests. In particular, it can be estimated as half of the drop of the force occurring at the displacement reversal point, as illustrated in [5]. Then, being the loading phase quasi-static, the Maxwell model is not active and the Kelvin model stiffness (k_0) can be obtained as the ratio between the maximum force attained just before the release (minus the friction force) and the maximum displacement (as reported in Table 1). Finally, the sum of the stiffness of the two models (k_0+k_1) can be set equal to the nominal stiffness of all HDRBs, equal to 0.62 kN/mm times the number of bearings (28). This way only the two damping constant c_1 and c_0 need to be calibrated using the displacement response. The obtained values are reported in Fig.6, together with the representation of the model and the physic variables of displacement u(t) and lost displacement $u_1(t)$, i.e. the global and internal variable of the model.

Fig.7 shows the comparison between the model data (red) and the experimental data (black) in terms global displacement, velocity, and acceleration Moreover, the lost displacement related to the Maxwell component $u_1(t)$ and the lost velocity $u_1(t)$' are also shown with blue lines. All the simulated response parameters are in good agreement with the measured ones, confirming the correctness of the model and permitting to interpretate the experimentally observed behavior of the base-isolated building. In fact, by observing Fig.7 it is evident that the displacement absorbed by the damper during the loading phase causes a viscous over-stresses during the release phase, leading the isolation system to oscillate around a non-zero displacement that decreases over-time.

Once the model is correctly calibrated from the push-and-release tests, the effective dynamic properties of the whole system are known, and it is possible to evaluate if the seismic response of the isolated building is in accordance with the design expectation.

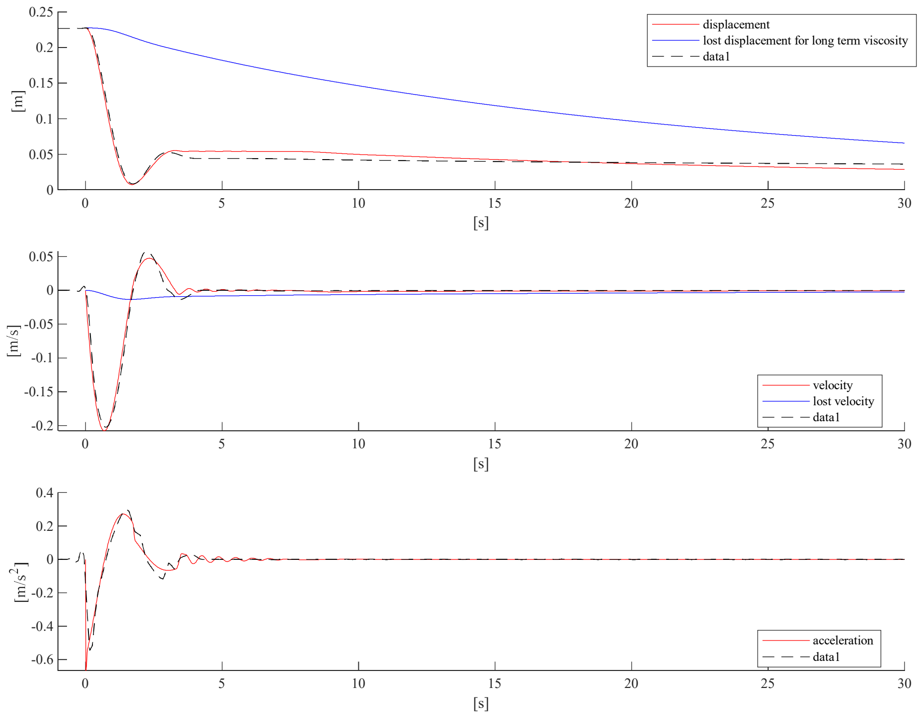

Fig. 7. Simulation of the response during the release phase of test D3

6 Conclusions

This article presented a brief overview of the experimental tests of a strategic base-isolated building, including quasi-static tests and as push-and release tests. The comparison between the experimental behaviour and the response of a simplified model is also presented. The magnitude of the maximum horizontal displacement achieved during the test is much larger than other similar tests documented up to date in the technical literature and close to the design displacement. Consequently, the presented tests can be considered as an experimental full-scale verification of the design procedure, the hybrid isolation system performance, and the installation process. In particular, the loading path of all the tests (except the first one), once subtracted the friction force and divided by the number of HDRBs, is in complete agreement with the one-side ramp test carried out on the single bearing (slow loading path). Conversely, it is significantly different from the Horizontal Cyclic Characteristic test (carried out at 0.5 Hz) due to the well-know viscous behavior of HDRBs. The displacement response of the isolation system recorded during the release phase of dynamic tests confirms the importance of the viscous contribution on the response of the HDRBs as well as the importance of the contribution of LFSBs on the response of the whole isolation system. In detail, the combined effect of the viscous displacement accumulated in the loading phase and the energy dissipated by the sliders, results in an high-damped cyclic behaviour oscillating around a non zero displacement. Moreover, the equilibrium reached immediately after a release test is not stable as the viscous over-stresses disappear and the residual displacement is slowly recovered over the time. All these effects have been properly simulated by the proposed analytical model, including a friction contribution simulating the LFSBs and two viscous contributions with two differet characteristic times simulating the HDRBs. This simple model can be very usfull to understand and interpretate similar tests carried out on base-isolated structures encompassing elastomeric bearings.

References

1. European Committee for Standardization (2009). EN 15129:2009 Antiseismic devices, European Committee for Standardization, Brussels.
2. European Committee for Standardization (2000). EN 1337-1:2000 Structural bearings – Part 1: General design rules, Brussels.
3. Micozzi F., Scozzese F., Ragni L., Dall'Asta A. (2022) Seismic reliability of base isolated systems: sensitivity to design choices. Engineering Structures 256, 114056
4. Dall'Asta, A., Leoni, G., Micozzi, F., Gioiella, L., Ragni, L. (2020). A resilience and robustness-oriented design of base-isolated structures: The New Camerino University Research Center. Frontiers in Built Environment 6, 50.
5. Dall'Asta A., Leoni G., Gioiella L., Micozzi F., Ragni L., Morici M., Scozzese F., Zona A. (2022) Push-and-release tests of a steel building with hybrid base isolation, Engineering Structures, vol. 272.
6. Dolce, M., Cardone, D., Croatto, F. 2005. Frictional behavior of steel-PTFE interfaces for seismic isolation. Bulletin of Earthquake Engineering 3, 75-99.
7. Abe, M., Yoshida, J., Fujino, Y. 2004. Multiaxial Behaviors of Laminated Rubber Bearings and Their Modeling. I: Experimental Study. Journal of Structural Engineering 130, 1119-1132.
8. Quaglini, V., Dubini, P., Vazzana, G. 2015. Experimental Assessment of High Damping Rubber Under Combined Compression and Shear. Journal of Engineering Material Technology 138, 011002.
9. Dall'Asta A. and L. Ragni (2006) Experimental tests and analytical model of high damping rubber dissipating devices, Engineering Structures, 28 (13), 1874-1884.
10. Ragni, L., Tubaldi, E., Dall'Asta, A., Ahmadi, H., Muhr, A. 2018b. Biaxial shear behaviour of HDNR with Mullins effect and deformation-induced anisotropy. Engineering Structures 154, 78-92.
11. Tubaldi, E., Ragni, L., Dall'Asta, A., Ahmadi, H., Muhr, A. 2017. Stress softening behaviour of HDNR bearings: modelling and influence on the seismic response of isolated structures. Earthquake Engineering and Structural Dynamics 46, 2033-2054
12. A. C. T. Thompson, A. S. Whittaker, G. L. Fenves, and S. A. Mahin (2000) Property modification factors for elastomeric seismic isolation bearings', in 12 WCEE 2000: 12th World Conference on Earthquake Engineering, Auckland, New Zeland: New Zealand Society for Earthquake Engineering.
    D. N. Grant, G. L. Fenves, and A. S. Whittaker (2004) Bidirectional modelling of high-damping rubber bearings, Journal of Earthquake Engineering, vol. 8, no. sup001, pp. 161–185.